Available online at www.sciencedirect.com
ScienceDirect
Remote Sensing of Environment 105 (2006) 299–312
Remote Sensing of Environment
www.elsevier.com/locate/rse

High-resolution image texture as a predictor of bird species richness

Véronique St-Louis [a,*], Anna M. Pidgeon [a], Volker C. Radeloff [a], Todd J. Hawbaker [a], Murray K. Clayton [b]

[a] Department of Forest Ecology and Management, University of Wisconsin – Madison, 1630 Linden Dr., Madison, WI, 53706, USA
[b] Department of Statistics, University of Wisconsin – Madison, 1300 University Ave., Madison, WI, 53706, USA

Received 19 December 2005; received in revised form 11 July 2006; accepted 15 July 2006

Abstract

We tested image texture as a predictor of bird species richness in a semi-arid landscape of New Mexico. Bird species richness was summarized from 10-min point counts conducted at 12 points within 42 plots (108 ha each) from 1996 to 1998. We calculated 14 first- and second-order texture measures in eight different window sizes on a set of digital orthophotos acquired in 1996. For each of the 42 plots, we summarized mean and standard deviation of each texture value within multiple window sizes. The relationship between image texture and average bird species richness was assessed using linear regression models. Single image texture measures such as the standard deviation described up to 57% of the variability in species richness. Coupling multiple measures of texture or coupling elevation with a single texture measure described up to 63% of the variability in bird species richness. Models incorporating two measures of texture and coarse habitat type described 76% of the variability in bird species richness. These results show that image texture analysis is a very promising tool for characterizing habitat structure and predicting patterns of species richness in semi-arid ecosystems. This method has several advantages over methods that rely on classified imagery, including cost-effectiveness, incorporation of within-habitat vegetation variability, and elimination of errors associated with boundary delineation.

Keywords: Image texture; Digital orthophotos; Species richness; Birds; Semi-arid ecosystems; Habitat structure; Biodiversity

1. Introduction

Global biodiversity is severely declining as a result of an unprecedented rate of species extinction (Pimm et al., 1995). The main cause for these extinctions is change in human land-use (Vitousek, 1994; Sala et al., 2000). The increasing pressure on ecosystems and its consequences on their integrity and patterns of biodiversity is a cause for growing concern. In order to develop effective management scenarios and identify areas of high conservation priority, patterns of biodiversity and the ecological drivers that create those patterns must be identified. Remote sensing is a great tool for this, especially if new techniques with greater accuracy and efficiency are developed.

The close link between land-use change and biodiversity mainly lies in the fact that land-use substantially modifies habitat structure. This results in shifts in habitat utilization following structure-altering disturbance, accompanied by changes in species occurrence patterns (e.g., Bolger et al., 1991). Habitat structure from fine- to broad-scales influences biodiversity. At a fine scale, vegetation structure has a strong impact on bird assemblages (Bersier & Meyer, 1994). At broader scales, landscape heterogeneity influences the spatial pattern of species richness for many taxonomic groups, including birds and amphibians (Atauri & de Lucio, 2001). Species' responses to land-use change and habitat structure (e.g., forest fragmentation) varies depending on their area requirements and ability to cross gaps (Dale et al., 1994). In this study, we developed methods to predict bird species richness, a measure of biodiversity, using habitat structure measures from remotely sensed data.

Bird communities are good indicators of biodiversity and habitat quality, partly because they encompass a wide range of niches and life-history requirements (Gregory et al., 2003). Birds are very sensitive to changes in habitat structure and composition; they respond strongly to fine-scale factors such as vegetation structure (Bersier & Meyer, 1994; Cody, 1981; MacArthur & MacArthur, 1961), and to broad-scale factors such as landscape composition and configuration (Villard et al.,

* Corresponding author. Tel.: +1 608 261 1050; fax: +1 608 262 9922.
E-mail address: vstlouis@wisc.edu (V. St-Louis).

0034-4257/$ - see front matter © 2006 Elsevier Inc. All rights reserved.
doi:10.1016/j.rse.2006.07.003

1999). Bird community composition can also be relatively easily assessed for small areas, since birds are identifiable by both auditory and visual cues, and standardized techniques exist (Bibby et al., 2000). However, monitoring avian communities on the ground is time consuming, and often limited to small spatial extents. Thus, detailed knowledge about biodiversity patterns at a regional level is expensive to obtain. One possible solution is to use remote sensing technologies because they cover broad spatial extents yet provide detailed attribute characterization (Wulder et al., 2004).

There are two main approaches to mapping spatial patterns of biodiversity using remote sensing (Nagendra, 2001; Turner et al., 2003): 1) direct mapping of species, and 2) indirect mapping of habitat via image classification. The direct mapping of species consists of mapping individual plants, or groups of plants, existing in spatially contiguous areas that can be distinguished by the remote sensor (Nagendra, 2001). Examples of direct mapping of species include mapping tree crowns using high-resolution imagery (Gougeon, 1995), or mapping king penguins (*Aptenodytes patagonicus*) using SPOT images in the southern Indian Ocean (Guinet et al., 1995). Another example includes mapping Adélie penguin rookeries using Landsat TM imagery in Antartica (Schwaller et al., 1989). Penguin rookeries show unique spectral signatures, which allow estimating rookery area and population size. These methods allow accurate mapping of species; however, they are mostly limited to large, colonial, or sessile organisms such as seabirds or trees.

The second method for mapping patterns of biodiversity using remote sensing is indirect mapping (Nagendra, 2001). It consists of predicting species distribution using habitat maps derived from remotely sensed data based on knowledge of habitat requirements, i.e., on-the-ground observation documenting the distribution and abundance of target species (Gottschalk et al., 2005). The remotely sensed imagery is classified into habitat classes that are important for a given species or species assemblage. For example, in a boreal agricultural-forest mosaic, landscape indices calculated from Landsat Thematic Mapper (TM) imagery are good predictors of bird species richness (Luoto et al., 2004). In a semi-arid landscape of New Mexico, land cover class area derived from Landsat TM imagery explains the pattern of black-throated sparrow (*Amphisphiza bilineata*) abundance and nest success (Pidgeon et al., 2003). Bird species distribution can also be predicted through the Gap Analysis Program (GAP) of the US Geological Survey (USGS), which involves the use of species range maps coupled with classified imagery and information on species habitat requirements derived from empirical data (Scott et al., 1996).

The use of cover classes to map species distributions and assemblages has three main limitations for our purposes. The first problem relates to the fact that traditional image classification methods often overlook within-habitat heterogeneity. This may not represent a problem where there is low variability within patches in a landscape, e.g., a landscape composed of distinct forest patches embedded in an agricultural matrix. However, where there is a high level of variability within cover types, e.g., in semi-arid landscapes, the lack of information on within-habitat variability is a major drawback.

The second potential problem of habitat classification relates to the difficulty of delineating boundaries at transition zones between different cover types, i.e., ecotones (Fortin et al., 2000). This uncertainty may be a significant source of error resulting in reduced classification accuracy, especially in areas where patches of several cover types with broad ecotones form a heterogeneous mosaic. Last, but not the least, image classification is a time-consuming and expensive process, particularly in habitats where extensive ground truthing is required to discriminate between different habitat types.

Other potential drawbacks associated with the use of classified imagery include: 1) a high variability in the land-cover maps derived from multiple independent classifications of the same area, and 2) an often poor correspondence between classified land cover and known species–habitat relationships.

A third way of mapping biodiversity, which has rarely been used yet addresses some of the aforementioned issues regarding the use of classified images, is to relate spectral radiance recorded from satellite sensors and species distribution obtained from field observation (Nagendra, 2001). The use of raw satellite imagery data to predict components of biodiversity has been attempted in several ecosystems and shows great promise. In the Sahel region of northern Senegal, a combination of the integrated vegetation index (iNDVI) and the landscape diversity index predicts bird species diversity well (Nøhr & Jørgensen, 1997). Other measures from Landsat Multispectral Scanner (MSS) and Landsat TM, such as Near Infrared reflectance (NIR) are significantly correlated with Dunlin (*Calidris alpina*) abundance (correlation between -0.79 and -0.68, $p<0.001$) in the Caithness region of Scotland (Lavers & Haines-Young, 1997). Dunlin abundance and distribution maps built from a model that incorporate NIR data are used to predict the impact of current land-use and conservation policies in the same area of Scotland (Lavers & Haines-Young, 1996). NDVI and short-wave infrared (band 5) derived from Landsat 7 Enhanced Thematic Mapper Plus (ETM+) effectively predict the regional occurrence of three species of warblers in Michigan (Laurent et al., 2005). Because it relates to vegetation greenness, NDVI is also used to assess habitat suitability for ungulates (hartebeest and wildebeest) and ostrich (*Struthio camelius*) in the Kalahari of Botswana (Verlinden & Masogo, 1997). Information from Landsat TM can be coupled with digital elevation models (DEM). In northeast Scotland, Aspinall and Veich (1993) used a Bayesian analysis approach to map Curlew (*Numenius arquata*) habitat by building relationships between the occurrence of Curlew and the Landsat bands and DEM values.

Since bird species richness and biodiversity are closely related to habitat structure (MacArthur, 1972; MacArthur & MacArthur, 1961), image-based measures of habitat heterogeneity (i.e., components of structure) may improve predictive models of species richness based on spectral values. Image texture may be a good measure of habitat heterogeneity. Considering the limitations associated with the use of classified imagery to predict patterns of biodiversity in some ecosystems, we developed new tools for monitoring species richness at broad scales based on unclassified, raw imagery.

Images are composed of tone (i.e., spectral information) and texture (i.e., tonal variability in a given area), two interdependent

characteristics (Baraldi & Parmiggiani, 1995; Harralick et al., 1973). The texture of an image contains important information about the spatial and structural arrangement of objects (Tso & Mather, 2001). There are two classes of texture measures: first-order (occurrence), and second-order (co-occurrence) statistics (Harralick et al., 1973; Mihran & Jain, 1998). First-order statistics are derived from the histogram of pixel intensities in a given neighborhood (i.e., a moving window), but ignore the spatial relationships of pixels. The standard deviation or mean of pixel values are examples of first-order measures (Mihran & Jain, 1998). Second-order statistics (e.g., angular second moment, entropy, sum of squares variance) are calculated from the grey-level co-occurrence matrix (GLCM), which indicates the probability that each pair of pixel values co-occur in a given direction and distance (Harralick et al., 1973; Mihran & Jain, 1998). The three second-order texture measures least correlated with each other are angular second moment, contrast, and correlation (Baraldi & Parmiggiani, 1995). These three statistics are consequently the most relevant for feature discrimination. Other methods used to calculate image texture include semi-variograms, Fourier transform, and fractal dimensions (Tso & Mather, 2001). In this study we focused on first- and second-order measures only.

The usefulness of first- and second-order statistics in the detection of structural patterns from satellite imagery has led to their application in image classification and segmentation (Franklin et al., 2000; Coburn & Roberts, 2004; Puissant et al., 2005). The angular second moment is used in surface pattern analysis of the boreal environment of eastern Canada (Peddle & Franklin, 1991). Second-order texture measures increase forest classification accuracy up to 77% when they are used to characterize forest objects from high-resolution imagery

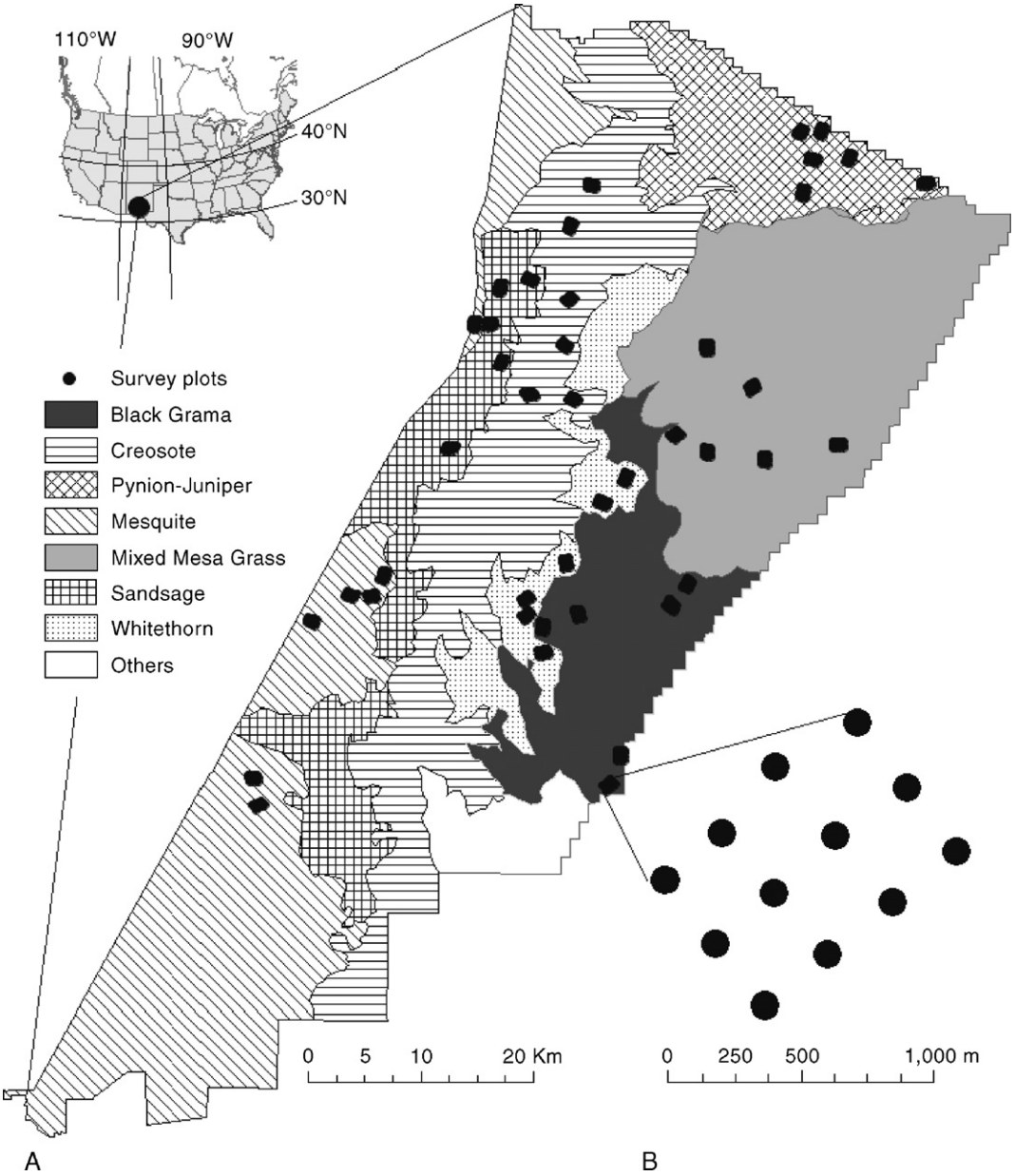

Fig. 1. A) Study area location, and B) study plot locations.

(Hay et al., 1996; Zhang et al., 2004). Texture measures predict up to 43% of the variability in hardwood forest leaf area index (LAI) in New Brunswick, Canada (Wulder et al., 1998). Image texture is also successful at distinguishing two different grassland management practices in Saskatchewan (Guo et al., 2004).

Although there have been a number of interesting applications of texture analysis for image classification, very few attempts have been made to explicitly assess the spatial heterogeneity of habitat and link image texture to other ecological variables. To our knowledge, Hepinstall and Sader (1997) were the first to integrate image texture, along with image spectral value, in a predictive model of bird occurrence. These authors found image texture to be useful in predicting the presence or absence of seven bird species (e.g., song sparrow (*Melospiza melodia*), yellow warbler (*Dendroica petechia*), black-throated green warbler (*Dendroica virens*)) in Maine. Six of the seven species were positively correlated with image texture. The common characteristic among the six species is their association with highly heterogeneous habitats. This suggests that image texture characterizes the heterogeneity in vegetation and habitat

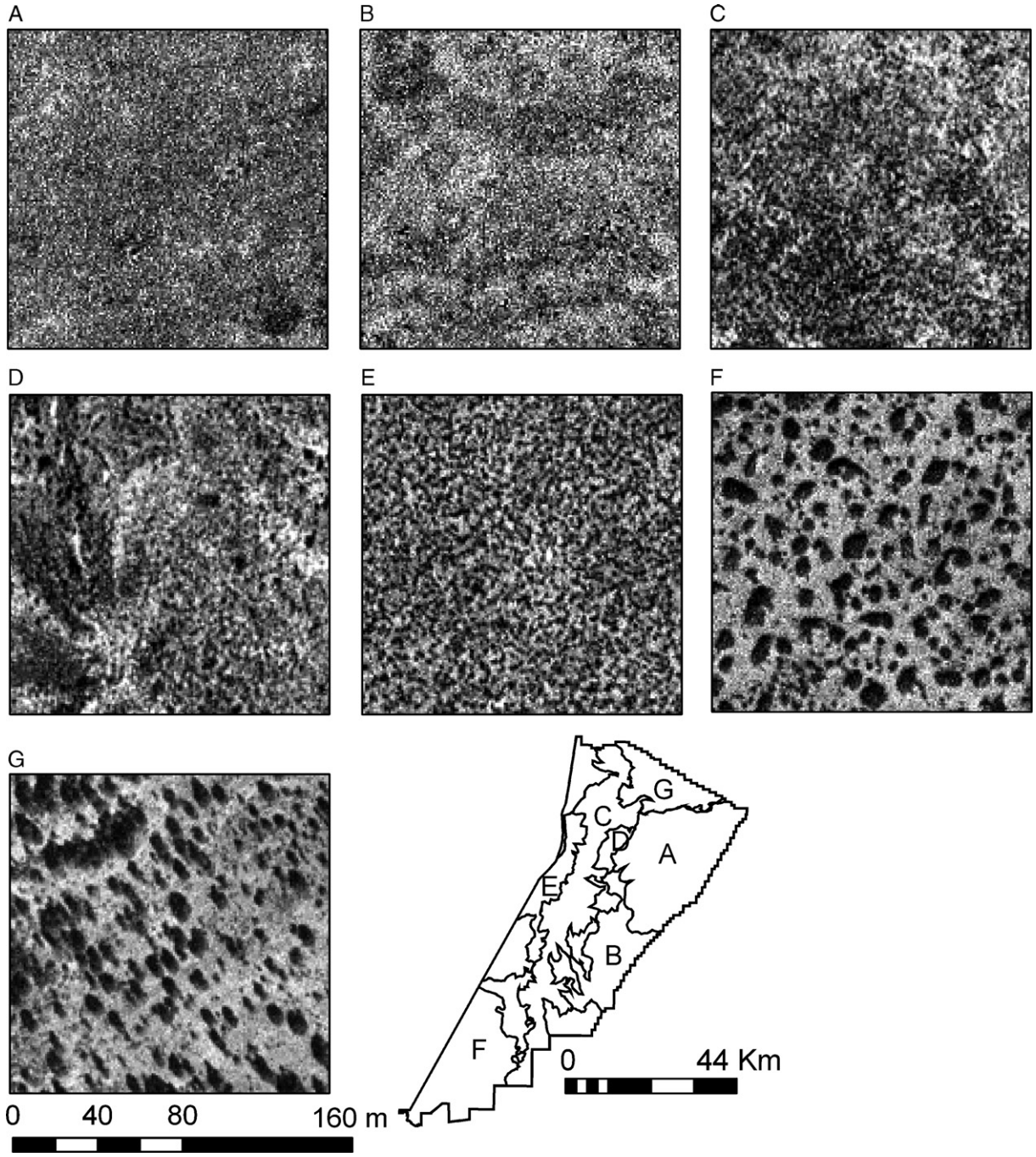

Fig. 2. DOQQs (1 m resolution) of the seven main habitat types: A) black grama, B) mesa grassland, C) creosote, D) whitetorn, E) sandsage, F) mesquite, and G) pinyon–juniper.

Table 1
Image texture acronym description and formulae

Type of measures	Texture measure	Formula*
1st order measures	Standard deviation	$SD = \sqrt{\frac{\sum_k (x_k-\mu)^2}{K}}$
		Where K=number of grey tone values μ=mean grey tone value
	Range	$RG = \max\{X\} - \min\{X\}$ Where $X = x_1, x_2, \ldots, x_k$
	Minimum	$MIN = \min\{X\}$
	Maximum	$MAX = \max\{X\}$
	Mean	$AVG = \frac{\sum_k x_k}{K}$
2nd order measures	Angular second moment	$ASM = \sum_i \sum_j \{p(i,j)\}^2$
		Where $p(i,j)$ is the (i,j)th entry of the normalized GLCM matrix,=$P(i,j)/R$, where R is a normalizing constant
	Contrast	$CON = \sum_{n=0}^{N-1} n^2 \left\{ \sum_{i=1}^{N} \sum_{\substack{j=1 \\ \lvert i-j\rvert=n}}^{N} p(i,j) \right\}$
	Correlation	$COR = \frac{\sum_i \sum_j (ij)p(i,j) - \mu_x \mu_y}{\sigma_x \sigma_y}$
		Where μ_x, μ_x, σ_x, and σ_y are the means and standard deviation of p_x and p_y − p_x and p_y are the marginal probabilities of x (entries in rows of normalized GLCM) and y (entries in columns)
	Dissimilarity	$DIS = \sum_{n=0}^{N-1} n \left\{ \sum_{i=1}^{N} \sum_{j=1}^{N} p(i,j) \right\}$
	Entropy	$ENT = -\sum_i \sum_j p(i,j) \log\,(p(i,j))$
	Information measures of correlation	$ICM1 = \frac{HXY - HXY1}{\max\{HX, HY\}}$
		$ICM2 = \sqrt{(1-\exp[-2.0(HXY2-HXY)])}$
		$HXY = -\sum_i \sum_j p(i,j) \log(p(i,j))$
		HX=entropy of p_x HY=entropy of p_y
		$HXY1 = -\sum_i \sum_j p(i,j) \log\{p_x(i)p_y(j)\}$
		$HXY2 = -\sum_i \sum_j p_x(i)p_y(j) \log\{p_x(i)p_y(j)\}$
	Inverse difference moment	$IDM = \sum_i \sum_j \frac{1}{1+(i-j)^2} p(i,j)$
	Sum of squares variance	$SSV = \sum_i \sum_j (i-\mu)^2 p(i,j)$

*From Harralick et al. (1973).

types, and can predict the occurrence of some species. No studies have yet quantified the relationship between image texture and species richness or other measures of biodiversity. This is unfortunate because the statistical properties of image texture measures suggest that they could be powerful tools to discriminate important habitat features for wildlife species, particularly for breeding birds, and to assess spatial patterns of biodiversity.

The main objective of our study was to evaluate image texture as a predictor of bird species richness in a grassland- and shrubland-dominated landscape. Specifically, we: 1) derived first- and second-order texture measures based on digital orthophoto quarter- quadrangles (DOQQs) at several scales, 2) evaluated the relationship between species richness and image texture using linear regression models, and 3) determined which window sizes and which statistical measures were the best predictors of species richness. Our approach using image textures to predict species richness avoids some of the potential drawbacks inherent in the use of classified remote sensing images (e.g., ignoring fine-scale heterogeneity, high time requirements), and fills the need for obtaining information on the spatial structure of habitat from raw images.

2. Data and methods

2.1. Study area

Our study was conducted on the McGregor Range of the Fort Bliss Military Reserve, which occupies 282,500 ha of the northern Chihuahuan Desert of New Mexico (Fig. 1A). The arid climate is characterized by average minimum and maximum temperatures for the May–July time period ranging from 11 to 19 °C and 30 to 35 °C respectively (Western Regional Climate Center, 2005). The average monthly precipitation for the same time period ranges between 13 and 44 mm. The elevation ranges from 1163 to 2332 m above sea level.

McGregor Range is characterized by seven main habitat types, which were obtained from a classification of vegetation types developed by Melhop et al. (1996) from multiple Landsat TM images. Major habitat types include two grasslands (black grama and mesa grassland), four shrublands (creosotebush, mesquite, sandsage, and whitethorn), and one tree-dominated (pinyon–juniper) habitat.

Black grama is dominated by black grama grass (*Bouteloua eriopoda*), with scattering of small shrubs, e.g., cane cholla (*Opuntia imbricata*) and *Yucca* spp. Mesa grassland is dominated by blue grama (*Bouteloua gracilis*), which occurs in combination with black grama, hairy grama (*Bouteloua hirsute*), and threeawn grass (*Aristida* spp.) among others. The

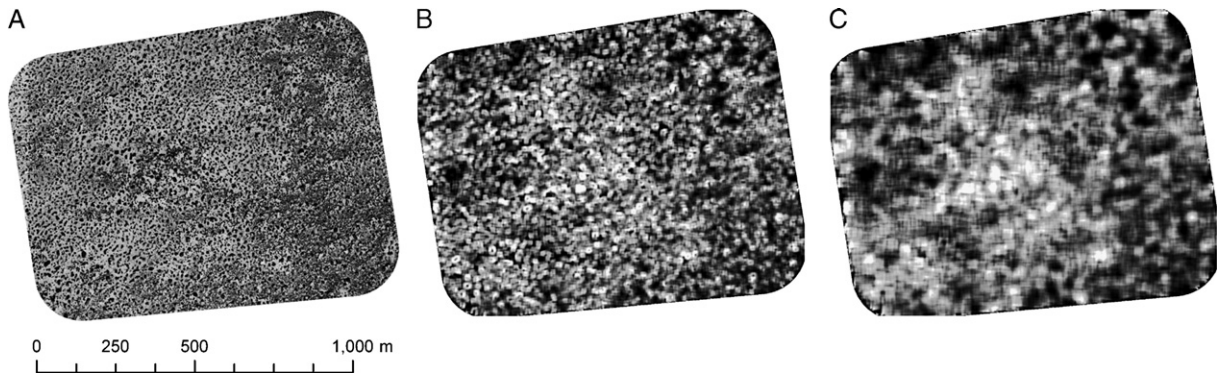

Fig. 3. Example of standard deviation filter applied to one of the 42 108-ha plots (A) with B) a 15×15 and C) a 31×31 moving window.

DOQQs of the black grama and mesa grasslands have very low contrast, i.e., low texture (Fig. 2A and B).

Creosote shrublands are dominated by creosote bush (*Larrea tridentata*), and are characterized by low shrub species richness and low ground cover. Creosote habitat exhibits more variability in grey tone values than the two grasslands, but is still fairly homogeneous with low ground cover (Fig. 2C). Whitethorn shrubland is dominated by whitethorn acacia (*Acacia constricta*), and several species of shrub and cacti. There is a wide range of grey tone values as well as high variability in the spatial distribution and clustering of grey tones in this habitat type (Fig. 2D). Sandsage habitat is dominated by the relatively dense shrub sand sagebrush (*Artemisia filifolia*), with many sub-dominants including soaptree yucca, little leaf sumac (*Rhus microphylla*), four-wing saltbush (*Atriplex canescens*), and mesquite. The DOQQs of sandsage exhibit high level of contrast induced by the different cover types, but very regular spatial distribution of grey tones (Fig. 2E). Mesquite shrublands are dominated by mesquite (*Proposis* spp.), occurring mainly as a multi-stemmed shrub which creates dunes by entrapping drifting sand (Hennessy et al., 1983). This shrubland includes a scattering of soaptree yucca (*Yucca elata*), broom snakeweed (*Gutierrezia sarothrae*), and other small shrubs in the interdunal area. This habitat type has very high texture in the DOQQs, with dark pixels representing the mesquite shrubs and bright pixels representing soil (Fig. 2F).

Finally, pinyon–juniper habitat is dominated by Colorado pinyon (*Pinyon edulis*), one-seed juniper (*Juniperus monosperma*), and alligator juniper (*Juniperus deppeana*). This habitat ranges from savanna, when there are fewer than 320 individual trees per hectare, to woodlands with an almost closed canopy (Dick-Peddie, 1993). This habitat exhibits the highest texture and contrast, and individual trees are visible (Fig. 2G). For more details on habitat types of the McGregor range, refer to Pidgeon et al. (2001, 2003), and Pidgeon (2000).

2.2. Bird data

Bird data were summarized over forty-two 108 ha plots between May 1 and June 7, 1996 through 1998 (Fig. 1B). Six plots were located randomly within each of the seven habitat classes with a surrounding buffer of at least 50 m of contiguous habitat (Pidgeon et al., 2003). Twelve points located 300 m apart in each plot were sampled four to five times a year by seven observers. Observers took part in an intensive training and calibration period prior to the field season. Plots were rotated among observers to avoid sampling bias. All birds seen or heard within 150 m of each point were recorded during 10-min periods. A 150 m distance is considered appropriate in open habitats (Martin et al., 1997). The tally of species from the 4–5 annual visits across the twelve points was used as a measure of species richness for each plot. We tested for and found no year effect on species richness (ANOVA for repeated measures; unpubl. data), and therefore used the average species richness in further analyses. An average of 24 species was detected at each of the 108 ha plot.

2.3. Image texture analysis

We calculated first- and second-order texture measures for each of the 42 plots based on USGS DOQQs with a spatial resolution of 1 m. Images were acquired in 1996. Although plot locations generally avoided roads, in a few instances minor dirt

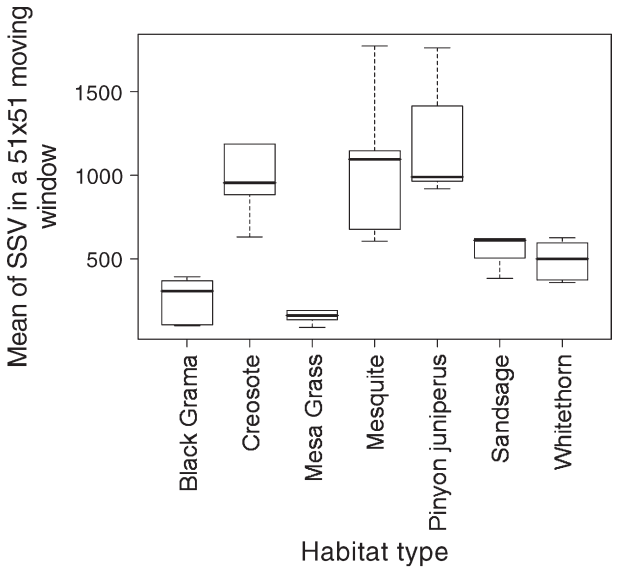

Fig. 4. Summary of image texture values across habitat types; example for mean sum of squares variance (SSV) in a 51×51 moving window. The horizontal bar represents the median, the box represents the first and third interquartiles, and the whiskers represent the range of data.

Table 2
Pearson correlation coefficients between the mean of first- and second-order texture measures calculated in the 3×3 moving window†

Measure type		1st order					2nd order							
	Texture	SD	RG	MIN	MAX	AVG	ASM	CON	COR	DIS	ENT	ICM1	IDM	SSV
1st order	SD††													
	RG	1.00***												
	MIN	–0.34*	–0.34*											
	MAX	0.64***	0.64***	0.51***										
	AVG	0.26	0.26	0.82***	0.91***									
2nd order	ASM†††	–0.88***	–0.88***	0.23	–0.62***	–0.29a								
	CON	0.96***	0.97***	–0.40**	0.56***	0.17	–0.76***							
	COR	0.42**	0.40**	–0.07	0.31*	0.19	–0.38a	0.27a						
	DIS	0.99***	1.00***	–0.36*	0.62***	0.23	–0.88***	0.98***	0.32*					
	ENT	0.88***	0.88***	–0.23	0.62***	0.29a	–1.00***	0.76***	0.38**	0.88***				
	ICM1	0.90***	0.90***	–0.23	0.63***	0.30*	–1.00***	0.78***	0.36*	0.89***	1.00***			
	IDM	–0.90***	–0.90***	0.23	–0.63***	–0.30a	1.00***	–0.79***	–0.32*	–0.90***	–1.00***	–1.00***		
	SSV	0.98***	0.98***	–0.38**	0.58***	0.20	–0.77***	0.99***	0.35*	0.97***	0.77***	0.7***	–0.79***	

Correlation levels were similar for the other window sizes.
† Significance codes: 0 '***' 0.001 '**' 0.01 '*' 0.05 'a' 0.1.
†† First-order texture measures: SD = standard deviation, RG = range, MIN = minimum, MAX = maximum, AVG = mean.
††† Second-order texture measures: ASM = angular second moment, CON = contrast, COR = correlation, DIS = dissimilarity, ENT = entropy, ICM1 = information measure of correlation 1, ICM2 = information measure of correlation 2, IDM = inverse difference moment, SSV = sum of squares variance.

roads fell within the plot boundaries. Roads were masked from the original images because we wanted the texture measures to represent habitat heterogeneity of the vegetation only. We calculated five first-order texture measures (minimum, mean, maximum, range and standard deviation; Table 1), using eight different moving window sizes, ranging from 3×3 to 101×101 pixels (e.g., Fig. 3). These window sizes were chosen to cover a wide range of sizes corresponding roughly to 9 m^2 to 10,000 m^2 on the ground. First-order texture measures were computed in ESRI® ArcGIS™ 9.1 (ESRI, 1999–2005).

We also calculated nine second-order texture measures, based on the GLCM (Harralick et al., 1973), using the same eight moving window sizes. Second-order measures were calculated in Matlab® 7.0.4.365 (TheMathWorks, Inc., 1984–2005) with the image processing toolbox, using the Condor® Project (http://www.cs.wisc.edu/condor/). The second-order measures considered were: angular second moment, contrast, dissimilarity, correlation, sum of squares variance, inverse difference moment, entropy, and information measures of correlation 1 and 2 (Table 1). With the exception of the information measures of correlation, the variables listed above are considered to be the most relevant texture measures for image classification (Baraldi & Parmiggiani, 1995). The texture measures were calculated in four directions (0°, 45°, 90° and 135°) and averaged, as suggested by Harralick et al. (1973).

For the fourteen texture measures, we obtained texture images at each of the 42 plots, in which each pixel contains texture information. We wanted to relate bird species richness with measures of image texture. To summarize the fourteen texture measures at each of the 108 ha study plots, we calculated two statistics: the mean and standard deviation of pixel values from the texture images. The mean calculates the average texture value at each plot, whereas the standard deviation is a measure of variability of texture for each of those plots. The mean and standard deviation of texture measures were used in the statistical analyses.

2.4. Statistical analyses

The relationship between species richness and texture measures was first assessed using univariate models that related the mean and standard deviation of each texture measure to species richness for each window size. We then used multiple regression models to predict species richness as a function of multiple texture measures. For the univariate linear models we conducted model selection based on the information theory approach of Burnham and Anderson (2002). For both the univariate and multiple regression models, we assessed how well the models performed using adjusted R^2 values. All statistical analyses were conducted in R 2.2.0 (R Development Core Team, 2005).

Table 3
Correlation between the different window sizes at which mean of first-order standard deviation was calculated

Window sizes	3x3	7x7	15x15	21x21	31x31	51x51	81x81	101x101
3x3								
7x7	0.95							
15x15	0.89	0.99						
21x21	0.88	0.98	1					
31x31	0.88	0.98	1	1				
51x51	0.87	0.98	1	1	1			
81x81	0.87	0.98	0.99	0.99	1	1		
101x101	0.87	0.97	0.99	0.99	1	1	1	

Lower diagonal indicates Pearson's correlation coefficient. All results are highly significant ($p<0.0001$).

Table 4
Results from univariate linear regression models relating species richness to single image texture at different moving window sizes

Summary statistic	Measure type	Texture measure	Window size								Best model AICc	Best model adjusted R^2	Best model p-value
			3×3	7×7	15×15	21×21	31×31	51×51	81×81	101×101			
Standard deviation	1st order†	SD					0.26	**0.36**	0.20		238.34	56.67	<0.001*
		RG			**0.57**						256.56	33.14	<0.001*
		MIN	0.42	0.19	**0.36**						257.35	31.87	<0.001*
		MAX	**0.26**	0.19			0.13	0.18			253.18	38.31	<0.001*
		AVG			**0.40**						245.50	48.62	<0.001*
	2nd order††	ASM	**0.52**								269.75	8.46	0.035
		CON	0.12	**0.26**	0.20	0.16	0.12				263.34	21.43	0.001
		COR			**0.68**	0.26					261.43	24.93	<0.001
		DIS		0.21	**0.33**	0.23	0.13				255.64	34.60	0.002
		ENT							0.39	**0.51**	264.45	19.32	<0.001
		ICM1					**0.75**				241.21	53.61	<0.001*
		ICM2				0.21	**0.30**	0.27			249.15	43.95	<0.001*
		IDM									†††		
		SSV						0.32	**0.40**	0.23	240.73	54.13	<0.001*
Mean of texture value	1st order	SD						0.15	0.27	**0.36**	260.61	26.37	<0.001*
		RG				0.10	0.12	0.16	0.22	**0.26**	264.01	20.17	<0.001
		MIN			0.11	0.14	0.17	**0.18**	0.18	0.18	264.43	19.36	<0.001
		MAX			**0.66**						265.47	17.33	0.004
		AVG											
	2nd order	ASM				0.10	0.12	0.16	0.26	**0.27**	264.90	18.44	0.003
		CON	0.13	0.13	0.13	0.12	0.13	0.12	0.12	**0.13**	270.22	7.44	0.044
		COR							0.28	**0.46**	259.44	28.40	<0.001
		DIS	0.13	0.13	**0.13**	0.12	0.13	0.12	0.12	0.13	269.51	8.99	0.030
		ENT							0.28	**0.38**	262.25	23.44	<0.001
		ICM1								**0.66**	254.80	35.88	<0.001*
		ICM2											
		IDM	0.13	0.12	0.13	0.12	**0.13**	0.12	0.13	0.12	269.77	8.43	0.035
		SSV							0.27	**0.43**	261.88	24.10	<0.001

Cell values represent the AICc w obtained for each individual window size for a given texture measure, for all models whose ΔAICc was smaller than 2. The AIC weight of the best moving window for a given texture is in bold. Correspondingly, values of AICc, adjusted R^2 and p-value are provided. The texture measures that best predicted species richness are underlined.

† First-order texture measures: SD = standard deviation, RG = range, MIN = minimum, MAX = maximum, AVG =mean.

†† Second-order texture measures: ASM = angular second moment, CON = contrast, COR = correlation, DIS = dissimilarity, ENT = entropy, ICM1 = information measure of correlation 1, ICM2 = information measure of correlation 2, IDM = inverse difference moment, SSV = sum of squares variance.

††† AICc is not shown for the models that were not significant from the linear regression analysis.

* Indicates cases where the model was still significant after Bonferonni correction (i.e., $p<0.0002$).

2.4.1. Image texture measures as predictors of species richness

2.4.1.1. Single measure of texture. The relationship between the mean and standard deviation of a given texture measure and species richness was assessed using univariate linear models for each window size. First, the corrected form of the Akaike's Information Criterion (AICc) was calculated for each fitted linear model (Hurvich & Tsai, 1989). The use of AICc is recommended for small sample sizes, specifically when the number of samples ($n=42$ in our case) divided by the number of parameters ($k=3$ for the univariate linear models) is smaller than 40. For a given texture measure (e.g., angular second moment), the window size that best predicted species richness was the one for which the univariate linear model exhibited the lowest AICc value. Second, models were compared using ΔAICc and AICc weights to evaluate if some window sizes are more successful than others at predicting species richness for a given texture measure. ΔAICc's between 0 and 2, and high AICc weights indicate strong support for those models relative to the other models considered (Burnham & Anderson, 2002). We tested for the presence of spatial autocorrelation in the residuals and found no spatial autocorrelation or spatial trend. Given the large number of univariate models fitted (i.e., 14 texture measures * two summary statistics * eight window size = 224 univariate models), we used the p-value as well as the Bonferonni adjusted p-value to evaluate the significance of the best univariate models. Using the Bonferonni correction, models are significant if the p-value is smaller than 0.0002 (i.e., 0.05/224).

2.4.1.2. Multiple texture measures. We fitted multiple regression models to evaluate the contribution of several texture measures in predicting species richness. For each of the eight window sizes, we first fitted a full model that contained the 27 possible texture measures (i.e., mean of the 13 measures (excludes ICM2) and standard deviation of the 14 measures). We also fitted a null model with the intercept only. We applied a stepwise selection algorithm starting with the null model, with a

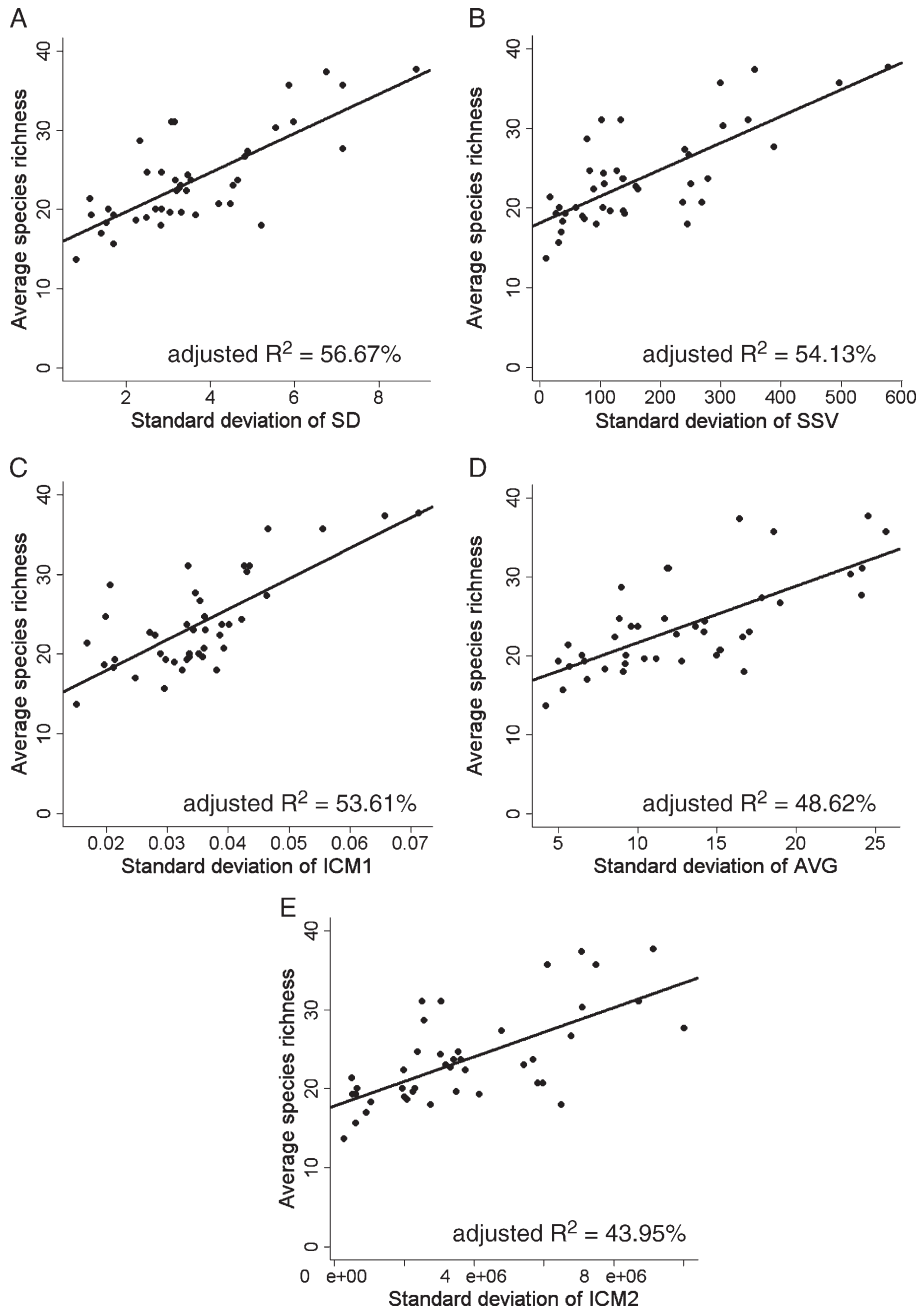

Fig. 5. Relationship between species richness and standard deviation of A) standard deviation in a 51×51 moving window, B) sum of squares variance in an 81×81 moving window, C) information measure of correlation 1 in a 31×31 moving window, D) mean in a 15×15 moving window and E) information measure of correlation 2 in a 31×31 moving window.

p-cutoff of 0.05 (Venables & Ripley, 2002). Specifying a null model as a starting point is more conservative than the usual method of starting with the full model. Using this method avoids some of the problems related to model over-fitting that could occur given the high correlations between the covariates present in the full model. The independent effect of each variable included in the final models was calculated using hierarchical partitioning (Chevan & Sutherland, 1991). We used hierarchical partitioning because we wanted to evaluate the relative importance of each texture measure retained after the stepwise regression for explaining bird species richness. The independent contribution of a given texture measure to explain variation in species richness is based on goodness of fit measures (i.e., R^2 in this case) calculated for all possible combinations of the texture measures that are retained after stepwise regression.

2.4.2. Inclusion of elevation and habitat type

We fitted a model that included habitat class alone as a predictor of species richness, as well as a second model that included habitat and different measures of texture from the multiple regression models. We compared those two multiple

regression models using an *F*-test. Also, because elevation gradient influences patterns of bird species richness (Rahbek, 1997), we included elevation variables in the best univariate and multiple regression models resulting from the aforementioned steps. Four elevation variables were calculated for each plot from a digital elevation model (DEM) with a 10 meter resolution: coefficient of variation (CV), mean, minimum and maximum elevation. The coefficient of variation is defined as the standard deviation divided by the mean.

3. Results

3.1. Descriptive statistics

Texture measures were highly variable among sites. Image texture also differed among the seven main habitat types identified from the classified image (Fig. 4). In general, texture increased from grasslands to shrublands to pinyon–juniper habitat.

Some of the texture measures were highly correlated (Table 2). For the 3×3 window size, nearly 25% of all possible pairwise comparisons had a positive correlation above 0.80, and 14% a negative correlation below −0.80. Note that the mean of information measure of correlation 2 did not appear in this correlation table because its value was equal to 0 for all plots. There was also high correlation between textures measured at different window sizes (Table 3). All the correlation coefficients were highly significant ($p<0.001$), but generally decreased as the difference between the size of the moving windows increased.

3.2. Relationship between image texture and species richness

3.2.1. Single measure of texture

First-order texture measures were all significant predictors of species richness except for the mean_{M} (Table 4) (subscripts indicate the mean (M) texture or the standard deviation (STDV) of texture). There was a positive and significant relationship between species richness and second-order measures of texture such as the $\text{sum of squares variance}_{STDV}$, and the information measures of correlation 1_{STDV} and 2_{STDV}. There was no significant model for the $\text{inverse difference moment}_{STDV}$. Models relating species richness to mean contrast, dissimilarity, and inverse difference moment were significant but had low R^2.

Many window sizes provided similar fit for a given measure of texture (Table 4). For example, a 51×51 window size provided the best model for $\text{first-order standard deviation}_{STDV}$ (AICc weight=0.36), but windows 31×31 and 81×81 gave similar good fits, as shown by their similar AICc weights (0.26 and 0.20 respectively). Only for a few measures was there a strong support for a given window size; for example, a 15×15 window for the range_{STDV}, the mean_{STDV}, and the maximum_{M}. For the other first-order texture measures, there were always at least two or three window sizes producing similar model fits.

Among the first-order texture measures, the $\text{first-order standard deviation}_{STDV}$ was the best predictor of species richness (Table 4). This measure alone explained 57% of the variability in species richness, followed by the mean_{STDV}, which explained 49% of the variation. Overall, standard deviation as a summary statistic for first-order texture measures gave better

Table 6
Comparison of the regression models with habitat type alone, multiple textures, and habitat type plus multiple textures as predictors of bird species richness

Model	Adjusted R^2	AICc	*p*-value
Richness ~ habitat	71.21	224.94	–
Richness ~ mean of $SSV^{*}_{31\times31}$ + standard deviation of $SD_{31\times31}$	61.78	234.26	–
Richness ~ mean of $SSV_{31\times31}$ + standard deviation of $SD_{31\times31}$ + habitat	76.28	218.32	0.015

The *p*-value is from the *F*-test comparing the model with habitat and texture to the model with habitat only.
* SD = standard deviation, SSV = sum of square variance.

Table 5
Results obtained from the linear regression models relating species richness to multiple measures of image texture at a given window size

Window Size	Intercept	Model parameters								AICc	Adj. R^2
		Mean			Standard deviation						
		CON	ICM1	SSV	COR	DIS	AVG	SD	SSV		
3×3	−541.27*,†		−167.41* (11)			8.49*** (54)			−0.11*** (35)	244.97	52.63
7×7	13.68***			−0.01** (21)			0.94*** (79)			242.34	53.89
15×15	4.67				94.77** (30)		0.62*** (70)			236.13	58.29
21×21	13.81***			−0.01 ** (22)				3.71*** (78)		234.04	62.16
31×31	14.18***			−0.01* (19)				3.46*** (81)		234.46	61.78
51×51	15.43***	−0.004* (11)						3.00*** (89)		236.37	60
81×81	15.18***							2.49*** (100)		239.48	55.48
101×101	15.41***							2.50**(100)		240.45	54.44

Values represent the coefficient of each parameter included in the final model after stepwise regression. A conservative *p*-cutoff of 0.05 was used as a threshold for variable inclusion. The numbers in parentheses indicate the percentage of independent effect that each variable have on the response calculated with the hierarchical partitioning method. The last two columns represent the AICc and adjusted R^2 values for the final models.
* AVG = mean, CON = contrast, COR = correlation, DIS = dissimilarity, ICM1 = information measure of correlation 1, SD = standard deviation, SSV = sum of square variance.
† Significance: <0.0001='***'; 0.001='**'; 0.01='*' 0.05 'a' 0.1.

results than the mean, as shown by smaller overall AICc values and higher adjusted R^2.

The second-order texture measures that best predicted species richness were the sum of squares variance$_{STDV}$, followed by the information measure of correlation 1 and 2$_{STDV.}$ These measures explained 54, 54, and 44% of the variation in species richness respectively. As with the first-order measures, the standard deviation of second-order texture measures was in general better than the mean as indicated by the lower AICc values and higher adjusted R^2.

Overall, the five best predictors of species richness from these univariate models were: 1) first-order standard deviation$_{STDV}$, 2) sum of squares variance$_{STDV}$, 3) information measure of correlation 1$_{STDV}$, 4) mean$_{STDV,}$ and 5) information measure of correlation 2$_{STDV}$ (Fig. 5). There was a positive relationship between the aforementioned measures and species richness. These variables explained 58, 55, 55, 50, and 45% respectively of the variability in species richness (Table 4). All of those models remained significant after Bonferonni correction.

3.2.2. Multiple regression models

Multiple measures of texture at a given scale of analysis explained a higher proportion of the variability in bird species richness than single measures (Table 5), with the exception of window sizes 81×81 and 101×101, where the best model selected with stepwise selection was the univariate one. Standard deviation$_{STDV}$ was included in five of the models and accounted for between 78 and 89% of the explained variation in species richness, using the hierarchical partitioning approach. Sum of square variance$_M$ was included in three of the models, and independently accounted for approximately 20% of the variability in species richness. For the 21×21 moving window, 62% of the variability was explained by two variables (Table 5) as opposed to 52% explained with the standard deviation$_{STDV}$ alone. For all listed best models, there were always other possible models giving similar adjusted R^2 values with different combination of variables. For example, for a 21×21 moving window, five other two variable models could provide an adjusted R^2 value between 58% and 62%. This suggests that some variables are interchangeable with little change in the model accuracy due to high correlation between variables.

3.3. Elevation and habitat

Habitat alone explained 71% of the variability in species richness (Table 6). This model was significantly better than the

Table 7
Results from multiple regression models combining elevation data with the five best predictors of species richness from Table 4

Model suite	Variable (txt)	AICc univariate regression	Adj. R^2 simple regression	Variable (elev.)	AICc texture+ elevation	Adjusted R^2 texture+ elevation	AICc w	*p*-value	Diff AICc **	Diff R^2
1	–	272.19 (intercept only)	–	**CV**	**250.67**	**41.88**	**0.99**	**<0.001**	**21.51**	–
	–		–	Max	261.5	24.81	0.004	<0.001	10.69	–
	–		–	Mean	262.84	22.36	0.002	<0.001	9.35	–
	–		–	Min	263.96	20.24	0.001	<0.001	8.23	–
2	Standard deviation of SD*** 51×5	238.34	56.67	**CV**	**233.16**	**62.95**	**0.43**	**0.01**	**5.18**	**6.28**
				Mean	234.80	61.47	0.19	0.02	3.54	4.80
				Min	235.14	61.16	0.16	0.02	3.20	4.49
				Max	234.46	61.78	0.22	0.02	3.88	5.11
3	Standard deviation of SSV 81×81	240.73	54.13	**CV**	**235.69**	**60.65**	**0.57**	**0.01**	**5.04**	**6.52**
				Max	238.08	58.34	0.17	0.04	2.65	4.21
				Mean	238.44	57.98	0.14	0.04	2.29	3.85
				Min	238.78	57.64	0.12	0.03	1.95	3.51
4	Standard deviation of ICM1 31×31	241.21	53.61	**CV**	**239.11**	**57.30**	**0.51**	**0.04**	**2.10**	**3.69**
				Max	241.13	55.20	0.19	0.13	0.08	1.59
				Mean	241.41	54.90	0.16	0.15	−0.20	1.29
				Min	241.68	54.61	0.14	0.18	−0.47	1.00
5	Standard deviation of AVG 15×15	245.50	48.62	**CV**	**242.68**	**53.51**	**0.31**	**0.03**	**2.82**	**4.89**
				max	242.96	53.20	0.27	0.03	2.54	4.58
				mean	243.24	52.89	0.23	0.04	2.26	4.27
				min	243.54	52.55	0.20	0.04	1.96	3.93
6	Standard deviation of ICM2 31×31	249.15	43.95	**CV**	**238.96**	**57.45**	**0.54**	**<0.001**	**10.19**	**13.50**
				max	240.92	55.42	0.20	<0.001	8.23	11.47
				mean	241.57	54.73	0.15	<0.001	7.58	10.78
				min	242.13	54.13	0.11	<0.001	7.02	10.18

Elevation variables are ranked in decreasing order based on the adjusted R^2 values for each suite. Multiple regression models including elevation and texture data are compared with univariate linear regression containing one of the five best measures of texture only. The elevation variables that most improved the univariate linear models are in bold. *P*-value corresponds to results from the likelihood-ratio test comparing the multiple versus the univariate linear regression models.

† AICc and adjusted R^2 of the univariate model including texture only.

†† Model 1 is for elevation only.

* AICc and adjusted R^2 of the model including texture and elevation covariate.

** Diff AICc = AICc univariate regression − AICc multiple regression.

*** SD = standard deviation, SSV = sum of squares variance, ICM1 = information measure of correlation, AVG = mean, ICM2 = information measure of correlation 2, CV = coefficient of variation.

model containing the intercept only (p-value<0.001). The inclusion of multiple measures of texture from the best multiple regression model at the 31×31 window size significantly improve this model, increasing explanatory power of the model to 76% of the variability in bird species richness. The addition of texture measures at other window sizes from the best multiple regression models (Table 5) did not significantly improve the model with habitat alone, but the p-values were close to 0.05 in some cases (e.g., 0.06 at the 21×21 moving window size). Elevation alone explained between 20 and 42% of the variation in species richness (Table 7). The elevation variable that best predicted species richness by itself was CV, with an AICc weight of 0.99. Adding CV significantly improved the univariate models containing single measures of texture. Mean elevation followed CV of elevation in improving the univariate models based on standard deviation of first-order measures. Maximum elevation followed CV of elevation in improving all other univariate models. Up to 63% of the variability in species richness was explained by a single measure of image texture (e.g., first-order standard deviation-$_{STDV}$) plus CV of elevation (Table 7). Only one measure of texture remained significant after inclusion of CV of elevation in the multiple regression models from Table 5, with the exception of the 15×15 window size. In that case, the adjusted R^2 increased from 58% to 62% with the inclusion of CV of elevation in the model. The addition of elevation did not significantly improve the multiple regression models.

4. Discussion

We found strong relationships between measures of image texture and bird species richness, providing evidence that important habitat features can be differentiated by surrogate measures such as image texture (Wulder et al., 1998). There was a particularly strong positive relationship between species richness and both first-order standard deviation and second-order variance. These two measures are highly correlated, and both represent a measure of vegetation spatial heterogeneity (Baraldi & Parmiggiani, 1995). Our results agree with previous work in Maine by Hepinstall and Sader (1997), where variance of image texture contributed to predict bird species associated with high habitat heterogeneity.

The standard deviation summary statistic of a number of texture measures (especially first-order standard deviation and sum of squares variance) was more strongly related to species richness than the mean of these texture measures. The standard deviation of texture measures at the plot level characterizes broad-scale variability in habitat structure. The positive relationship between the plot-level standard deviation of image texture and species richness provides support for the theory that habitat heterogeneity determines species richness and can be characterized at multiple scales (Noss, 1990). Habitats with a large amount of heterogeneity in their spectral signature at the scales of both the moving window and the plot thus appear to satisfy the life-history requirements of more species (i.e., higher number of available niches). Because our measures described the variability of the vegetation among and within habitat types these results suggest that image texture analysis can predict avian species richness well in this ecosystem.

We did not find a consistent pattern regarding which window size best predicts species richness for several possible reasons. First, the species present in this ecosystem occupy territories of varying sizes which may blur the effect of the scale of analysis for determining species richness. For example, the loggerhead shrike (*Lanius ludovicianus*) defends larger territories than other passerine birds of similar body size; territory size varies depending on the geographic location, but may range from 3 to 25 ha (Yosef, 1996). In contrast, the black-throated sparrow (*Amphispiza bilineata*) defends much smaller territories which may range from 0.89 to 2.36 ha in New Mexico (Johnson et al., 2002). The lack of a single best window size may also be due to the fact that the spectrum of window sizes chosen does not provide distinct information, as shown by the high correlation of texture across window sizes. This suggests that further work should be conducted to evaluate the contribution of texture calculated in more "extreme" window sizes in explaining species richness, or to conduct similar studies in landscapes where texture varies more across scales. Also, since birds may respond to habitat features beyond their home range, one could consider calculating image texture to include areas outside the plot. In this study, however, we purposely chose to calculate texture uniquely at the plot level to understand the effect of within-plot structural variability on bird species richness.

Habitat type from a Landsat image classification was a strong predictor of species richness. In McGregor Range, Pidgeon et al. (2001) found that species richness was very different among habitat types, significantly declining from pinyon–juniper to shrublands to grasslands, which corresponds to a decline in habitat spatial heterogeneity. Adding multiple image texture measures to a univariate habitat type model increased predictive power, capturing 76% of variability in species richness. This suggests that fine-scale habitat variability is important in determining patterns of species richness in our study area. The strong relationship between species richness and image texture suggests also that image texture analysis is suitable for characterizing differences in habitat heterogeneity that determine spatial patterns of species richness across the landscape.

We found a positive relationship between the four elevation variables and species richness, in agreement with previous research regarding the importance of elevation gradient in determining bird species richness (Hawkins, 1999; Rahbek, 1997). The coefficient of variation in elevation was particularly strong in predicting species richness. Over the spatial extent considered (i.e., 108 ha) variability in elevation may promote variability in available resources and diversity of niches for breeding bird species.

Our results show that a univariate first-order measure such as standard deviation calculated from DOQQs predicts species richness well. This is an advantage because first-order texture measures are relatively fast to compute, as opposed to second-order measures which require more computing-intensive algorithms.

However, the multiple regression models do suggest that second-order measures also help to explain variability in species

richness. Second-order measures take into account the spatial relationships between pixel values, which may be an important aspect of bird habitat quality. For example, the distribution of escape cover across an area may influence species richness. This spatial aspect of habitat suitability can only be reflected in second-order texture measures.

Our work clearly shows strong correlation between image texture and species richness. At this point, however, we can only speculate on the ecological significance of this relationship, and future work is needed to understand the relevance of complex texture measures (e.g., second-order measures) for determining species richness. From our results, we can hypothesize that, at the scale of the moving window, high first-order standard deviation or sum of squares variance represents a heterogeneous distribution of plants. This high-level of local variability in plant composition and/or structure can support a larger number of bird species (Rotenberry, 1985).

Our results suggest that image texture can act as surrogate for habitat structure, and is a promising tool for predicting patterns of species richness. This approach represents a cost-effective way of mapping habitat heterogeneity and species richness compared to the traditional method of classifying images. Most texture measures can be easily calculated and algorithms to do so are an integral part of most remote sensing software.

Image texture has potential utility far beyond predicting species richness in semi-arid ecosystems. It may be useful to model species richness in forest ecosystems, where it can capture within-forest variability, as shown by Hepinstall and Sader's (1997) study in Maine. Quantifying landscape heterogeneity based on continuous data is one of the main challenges of landscape ecologists today (Turner, 2005); image texture can be used in accomplishing this task.

5. Conclusion

Mapping broad-scale patterns of species richness is a major challenge. There are drawbacks to using traditional remote sensing techniques based on classified images in ecosystems where the boundary between some habitat types is not clearly defined, as is the case in the northern Chihuahuan Desert. Our study describes a novel application of image texture analysis to mapping and understanding species richness patterns in semi-arid ecosystems. Three main conclusions can be drawn from our study. First, both first- and second-order texture measures were strong predictors of species richness and the relationships were robust across window sizes. Second, environmental factors such as coefficient of variation in elevation and habitat type significantly improved the models when used in conjunction with texture measures. Finally, models that included multiple texture measures explained more variability in species richness than univariate models. Our results suggest that image texture offers a promising, cost-effective metric for mapping species richness in semi-arid ecosystems. Future work is needed to evaluate the possibility of extending these results to other ecosystems, and using high-resolution satellite imagery for texture calculation.

Acknowledgements

We would like to thank Dallas Bash for technical support, Brian Locke for ecological insights and making our research on Fort Bliss possible, and Bill Taylor from the Computer Science department at UW-Madison for his help in computing second-order texture measures. We thank James D. Forester, Shelley L. Schmidt, Edward J. Laurent and two anonymous reviewers for valuable comments on previous versions of this manuscript, and all field assistants who collected bird data. We gratefully acknowledge support by the Strategic Environmental Research and Development Program. Acquisition of bird data was supported by the U.S. Department of Defense Legacy Resource Management Program, Ft. Bliss Directorate of Environment, USGS BRD Texas Cooperative Fish and Wildlife Research Unit, USGS BRD Wisconsin Cooperative Wildlife Research Unit, and the Department of Wildlife Ecology at the University of Wisconsin–Madison.

References

Aspinall, R., & Veich, N. (1993). Habitat mapping from satellite imagery and wildlife survey data using a Bayesian modeling procedure in a GIS. *Photogrammetric Engineering and Remote Sensing*, *59*, 537−543.

Atauri, J. A., & de Lucio, J. V. (2001). The role of landscape structure in species richness distribution of birds, amphibians, reptiles and lepidopterans in Mediterranean landscapes. *Landscape Ecology*, *16*, 147−159.

Baraldi, A., & Parmiggiani, F. (1995). An investigation of the textural characteristics associated with gray level cooccurrence matrix statistical parameters. *IEEE Transactions on Geoscience and Remote Sensing*, *33*, 293−304.

Bersier, L. F., & Meyer, D. R. (1994). Bird assemblages in mosaic forests: The relative importance of vegetation structure and floristic composition along successional gradient. *Acta Oecologia*, *15*, 561−576.

Bibby, C. J., Burgess, N. D., Hill, D. A., & Mustoe, S. (2000). *Bird census techniques* (2nd Edition) London: Academic Press.

Bolger, D. T., Alberts, A. C., & Soulé, M. E. (1991). Occurrence patterns of bird species in habitat fragments: Sampling, extinction, and nested species subsets. *The American Naturalist*, *137*, 155−166.

Burnham, K. P., & Anderson, D. R. (2002). *Model selection and multimodel inference: a practical information—theoretic approach* (pp. 60−77). New York: Springer.

Chevan, A., & Sutherland, M. (1991). Hierarchical partitioning. *The American Statistician*, *45*, 90−96.

Coburn, C. A., & Roberts, A. C. B. (2004). A multiscale texture analysis procedure for improved forest stand classification. *International Journal of Remote Sensing*, *25*, 4287−4308.

Cody, M. L. (1981). Habitat selection in birds: The roles of vegetation structure, competitors, and productivity. *BioScience*, *31*, 107−113.

Dale, V. H., Pearson, S. M., Offerman, H. L., & O'Neill, R. V. (1994). Relating patterns of land-use change to faunal biodiversity in the Central Amazon. *Conservation Biology*, *8*, 1027−1036.

Dick-Peddie, W. A. (1993). *New Mexico vegetation: past, present, and future* (pp. 87−90). Albuquerque: University of New Mexico Press.

ESRI (Environmental Systems Research Institute). (1999–2005). *Arc GIS. Release 9.1. ESRI* Redlands, California, USA.

Fortin, M. J., Olson, R. J., Ferson, S., Iverson, L., Hunsaker, C., Edwards, G., et al. (2000). Issues related to the detection of boundaries. *Landscape Ecology*, *15*, 453−466.

Franklin, S. E., Hall, R. J., Moskal, L. M., Maudie, A. J., & Lavigne, M. B. (2000). Incorporating texture into classification of forest species composition from airborne multispectral images. *International Journal of Remote Sensing*, *21*, 61−79.

Gottschalk, T. K., Huettmann, F., & Ehlers, M. (2005). Thirty years of analysing and modelling avian habitat relationships using satellite imagery data: A review. *International Journal of Remote Sensing*, *26*, 2631−2656.

Gougeon, F. A. (1995). Comparison of possible multispectral classification schemes for tree crown individually delineated on high spatial resolution MEIS images. *Canadian Journal of Remote Sensing*, *21*, 1−9.

Gregory, R. D., Noble, D., Field, R., Marchant, J., Raven, M., & Gibbons, D. W. (2003). Using birds as indicators of biodiversity. *Ornis Hungarica*, *12–13*, 11−24.

Guinet, C., Jouventin, P., & Malacamp, J. (1995). Satellite remote sensing in monitoring change of seabirds: Use of Spot image in king penguin population increase at Ile aux cochons, Crozet Archipelago. *Polar Biology*, *15*, 511−515.

Guo, X., Wimshurst, J., McCanny, S., Fargey, P., & Richard, P. (2004). Measuring spatial and vertical heterogeneity of grasslands using remote sensing techniques. *Journal of Environmental Informatics*, *3*, 24−32.

Harralick, R. M., Shanmugam, K., & Dinstein, I. (1973). Textural features for image classification. *IEEE Transactions on Systems, Man, and Cybernetics*, *SMC-3*, 610−621.

Hawkins, A. F. A. (1999). Altitudinal and latitudinal distribution of east Malagasy forest bird communities. *Journal of Biogeography*, *26*, 447−458.

Hay, G. J., Niemann, K. O., & McLean, G. (1996). An object-oriented image-texture analysis of H-resolution forest imagery. *Remote Sensing of the Environment*, *55*, 108−122.

Hennessy, J. T., Gibbens, R. P., Tromble, J. M., & Cardenas, M. (1983). Vegetation changes from 1935 to 1980 mesquite dunelands and former grasslands of southern New Mexico. *Journal of Range Management*, *36*, 370−374.

Hepinstall, J. A., & Sader, S. A. (1997). Using bayesian statistics, thematic mapper satellite imagery, and breeding bird survey data to model bird species probability of occurrence in Maine. *Photogrammetric Engineering & Remote Sensing*, *63*, 1231−1237.

Hurvich, C. M., & Tsai, C. L. (1989). Regression and time series model selection in small samples. *Biometrika*, *76*, 297−307.

Johnson, M.J., Van Riper III, C., Pearson, K.M. (2002). Black-throated sparrow (*Amphispiza bilineata*). *The Birds of North America, No. 637*, The Academy of Natural Sciences, Philadelphia, and The American Ornithologists' Union, Washington, D.C.

Laurent, E. J., Shi, H., Gatziolis, D., LeBouton, J. P., Walters, M. B., & Liu, J. (2005). Using the spatial and spectral precision of satellite imagery to predict wildlife occurrence patterns. *Remote Sensing of the Environment*, *97*, 249−262.

Lavers, C., & Haines-Young, R. (1996). Using models of bird abundance to predict the impacts of current land-use and conservation policies in the flow country of Caithness and Sutherland, northern Scotland. *Biological Conservation*, *75*, 71−77.

Lavers, C., & Haines-Young, R. (1997). The use of satellite imagery to estimate *Dunlin Calidris* alpina abundance in Caithness and Sutherland and in the Shetland Islands. *Bird Study*, *44*, 220−226.

Luoto, M., Virkkala, R., Heikkinen, R., & Rainio, K. (2004). Predicting bird species richness using remote sensing in boreal agricultural-forest mosaics. *Ecological Applications*, *14*, 1946−1962.

MacArthur, R. H. (1972). *Geographical ecology: Patterns in the distribution of species.* New York: Harper and Row.

MacArthur, R. H., & MacArthur, J. W. (1961). On bird species diversity. *Ecology*, *42*, 594−598.

Martin, T. E., Paine, C., Conway, C. J., Hochachka, W. M., Allen, P., & Jenkins, W. (1997). *BBird field protocol.* Missoula, Montana, USA: University of Montana.

Melhop, P., Muldavin, E., Bennett, T., Wood, S., Yanoff, S., Douglas, N., et. al. (1996). Vegetation of Fort Bliss, Texas and New Mexico, Final report. Volume II; Vegetation map. *New Mexico Natural Heritage Program, Biology Dept., University of New Mexico, Albuquerque, New Mexico, USA*.

Mihran, T., & Jain, A. K. (1998). Texture analysis. In C. H. Chen, L. F. Pau, & P. S. P. Wang (Eds.), *The handbook of pattern recognition and computer vision,* (pp. 207−248). Word Scientific Publishing Co.

Nagendra, H. (2001). Using remote sensing to assess biodiversity. *International Journal of Remote Sensing*, *22*, 2377−2400.

Nøhr, H., & Jørgensen, A. F. (1997). Mapping of biological diversity in Sahel by means of satellite image analyses and ornithological surveys. *Biodiversity and Conservation*, *6*, 545−566.

Noss, R. F. (1990). Indicators for monitoring biodiversity: A hierarchical approach. *Conservation Biology*, *4*, 355−364.

Peddle, D., & Franklin, S. (1991). Image texture processing and data integration for surface pattern discrimination. *Photogrammetric Engineering and Remote Sensing*, *57*, 413−420.

Pidgeon, A. M. (2000). Avian abundance and productivity at the landscape scale in the Northern Chihuahuan Desert. Dissertation. University of Wisconsin–Madison, Madison, Wisconsin, USA.

Pidgeon, A. M., Mathews, N. E., Benoit, R., & Nordheim, E. V. (2001). Response of avian communities to historic habitat change in the Northern Chihuahuan Desert. *Conservation Biology*, *15*, 1772−1788.

Pidgeon, A. M., Radeloff, V. C., & Mathews, N. E. (2003). Landscape-scale patterns of black-throated sparrow (*Amphispiza bilineata*) abundance and nest success. *Ecological Applications*, *13*, 530−542.

Pimm, S. L., Russel, G. J., Gittleman, J. L., & Brooks, T. M. (1995). The future of biodiversity. *Science*, *269*, 347−350.

Puissant, A., Hirsch, J., & Weber, C. (2005). The utility of texture analysis to improve per-pixel classification for high to very high spatial resolution imagery. *International Journal of Remote Sensing*, *26*, 733−745.

R Development Core Team. (2005). *R: A language and environment for statistical computing.* Vienna, Austria: R Foundation for Statistical Computing.

Rahbek, C. (1997). The relationship among area, elevation, and regional species richness in neotropical birds. *The American Naturalist*, *149*, 875−902.

Rotenberry, J. T. (1985). The role of habitat in avian community composition: Physiognomy or floristic? *Oecologia*, *67*, 213−217.

Sala, O. E., Chapin, F. S. I., Armesto, J. J., Berlow, E., Bloomfield, J., Dirzo, R., et al. (2000). Global biodiversity scenarios for the year 2100. *Science*, *287*, 1770−1774.

Schwaller, M. R., Olson, Jr., C.E., Ma, Z., Zhu, Z., & Dahmer, P. (1989). A remote sensing analysis of Adélie penguin rookeries. *Remote Sensing of Environment*, *28*, 199−206.

Scott, J. M., Tear, T. H., & Davis, F. W. (1996). *Gap analysis: A landscape approach to biodiversity planning.* Bethesda: American Society for Photogrammetry and Remote Sensing.

TheMathWorks, Inc. (1984–2005). *Matlab.* Natik, MA, USA.

Tso, B., & Mather, P. M. (2001). *Classification methods for remotely sensed data* (pp. 186−229). New York: Taylor & Francis.

Turner, M. G. (2005). Landscape ecology in North America: Past, present, and future. *Ecology*, *86*, 1967−1974.

Turner, W., Spector, S., Gardiner, N., Fladeland, M., Sterling, E., & Steininger, M. (2003). Remote sensing for biodiversity science and conservation. *Trends in Ecology and Evolution*, *18*, 306−314.

Venables, W. N., & Ripley, B. D. (2002). *Modern applied statistics with S* (pp. 175−176). New York: Springer.

Verlinden, A., & Masogo, R. (1997). Satellite remote sensing of habitat suitability for ungulates and ostrich in the Kalahari of Botswana. *Journal of Arid Environments*, *35*, 563−574.

Villard, M. -A., Trzcinski, M. K., & Merriam, G. (1999). Fragmentation effects on forest birds: relative influence of woodland cover and configuration on landscape occupancy. *Conservation Biology*, *13*, 774−783.

Vitousek, P. M. (1994). Beyond global warming: Ecology and global change. *Ecology*, *75*, 1861−1876.

Western Regional Climate Center. Orogrande 1N New Mexico. Western Regional Climate Center, Reno, Nevada. Available from http://www.wrcc.dri.edu. Accessed 2005 Dec 8.

Wulder, M. A., Hall, R. J., Coops, N. C., & Franklin, S. E. (2004). High spatial resolution remotely sensed data for ecosystem characterization. *BioScience*, *54*, 511−521.

Wulder, M. A., LeBrew, E. F., Franklin, S. E., & Lavigne, M. B. (1998). Aerial image texture information in the estimation of northern deciduous and mixed wood forest leaf area index (LAI). *Remote Sensing of Environment*, *64*, 64−76.

Yosef, R. (1996). Loggerhead shrike (*Lanius ludovicianus*).The Birds of North America, NO 231, The Academy of Natural Sciences, Philadelphia, and The American Ornithologists' Union, Washington, D.C.

Zhang, C., Franklin, S. E., & Wulder, M. A. (2004). Geostatistical and texture analysis of airborne-acquired images used in forest classification. *International Journal of Remote Sensing*, *25*, 859−865.